

Behavior of colloidal particles at an air/nematic liquid crystal interface

M.A. Gharbi,¹ M. Nobili,^{1,*} M. In,¹ G. Prévot,¹ P. Galatola,² JB. Fournier,² and Ch. Blanc^{1,†}

¹*Laboratoire des Colloïdes, Verres et Nanomatériaux(LCVN),
UMR5587 CNRS and Université Montpellier II, Place Eugène Bataillon, 34095 Montpellier, France.*

²*Laboratoire Matière et Systèmes Complexes (MSC),
UMR 7057 CNRS and Université Paris Diderot-Paris 7, CC 7056, 75205 Paris, France.*

(Dated: November 9, 2018)

We examine the behavior of spherical silica particles trapped at an air-nematic liquid crystal interface. When a strong normal anchoring is imposed, the beads spontaneously form various structures depending on their area density and the nematic thickness. Using optical tweezers, we determine the pair potential and explain the formation of these patterns. The energy profile is discussed in terms of capillary and elastic interactions. Finally, we detail the mechanisms that control the formation of an hexagonal lattice and analyze the role of gravity for curved interfaces.

PACS numbers: 61.30.Jf,61.30.Hn,64.75.Xc

Colloidal particles confined at liquid interfaces display rich two-dimensional (2D) phase properties [1, 2]. The spontaneous formation of ordered structures such as microcrystals has been mainly studied in simple fluids [3–5] where the self-arrangement is controlled by direct colloidal interactions (electrostatic [6, 7], magnetic [1]...) and possible capillary effects. The latter might come from the anisotropic shape [8] or the roughness of the particles [9]. It is only recently that an interest [10–13] has developed in the behavior of particles trapped at an ordered fluid interface. In bulk liquid crystals (LC), additional long-range interactions between particles are present because of the partial order and elasticity. Colloidal suspensions [14, 15] in a nematic matrix are thus qualitatively different from their isotropic analogues. They display rich self-ordering phenomena involving particles and topological defects. At LC interfaces, complex ordered structures were also observed in several cases: glycerin droplets [10, 11] or solid beads [16] at nematic/air interfaces or microparticles at nematic/water interface [12, 13]. All these systems display 2D hexagonal crystals that were ascribed to the competition between a repulsion due to the bulk liquid crystal elasticity and a capillary attraction resulting from the interface distortions caused by the “nematic elastic pressure”. This new type of capillary interaction is however thoroughly discussed in two recent works [17, 18] and its role is not clearly established. To clarify the respective role of the elastic and capillary force a direct force measurement between trapped particles coupled with a careful control of the LC anchoring on the beads as well as of the flatness of interface would be suitable.

In this work, we present a simple technique for trapping colloids at the flat interface of an aligned thin layer of nematic liquid crystal. By controlling the beads density, the interface curvature and the LC anchoring, we were then able to establish their respective role in the formation of the colloidal structures. A direct measurement of the pairwise interaction has been obtained with

optical tweezers, which allowed us to discuss the respective roles played by LC elasticity and capillarity.

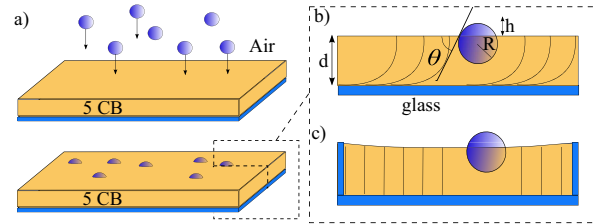


FIG. 1: a) Deposition of colloids at the air liquid crystal interface. The LC texture is either hybrid due to the strong planar anchoring on polyimide and homeotropic at the air (1-b) or fully homeotropic on silanized glass (1-c).

The studied systems are obtained by trapping solid spheres at the interface between air and a nematic LC at 21°C. Aggregates of dry silica beads (radius $R = 1.96\mu\text{m}$ from Bangslabs) are “exploded” by an air pulse in a box. The individual spheres then gently settle on a liquid crystal slab (fig. 1) which avoids the presence of colloids in bulk. The LC layer (thickness in the range 10-100 μm) is obtained by spin coating 4-pentyl-4-cyanobiphenyl (5CB from Synthron) on a glass slide treated with polyimide (EHC Japan) that ensures a strong planar anchoring. The layer exhibits a hybrid texture due to the strong homeotropic anchoring at the air interface (fig. 1-b). Homogeneous homeotropic layers have also been studied by using a silane treatment on glass with N,N-dimethyl-N-octadecyl-3amininopropyl trimethoxysilyl chloride (DMOAP from Aldrich) but the poor wettability of 5CB on silanized surfaces requires using a surrounding glass wall as shown in Fig. 1-c. Note finally that the beads -initially dispersed in water- were covered with a monolayer of DMOAP following Ref. [19], which ensures a strong homeotropic surface anchoring on 5CB. They were then dried at $T = 110^\circ\text{C}$ before use [20].

The colloids/LC systems were observed in transmission mode under a polarizing microscope (LEICA DM 2500 P)

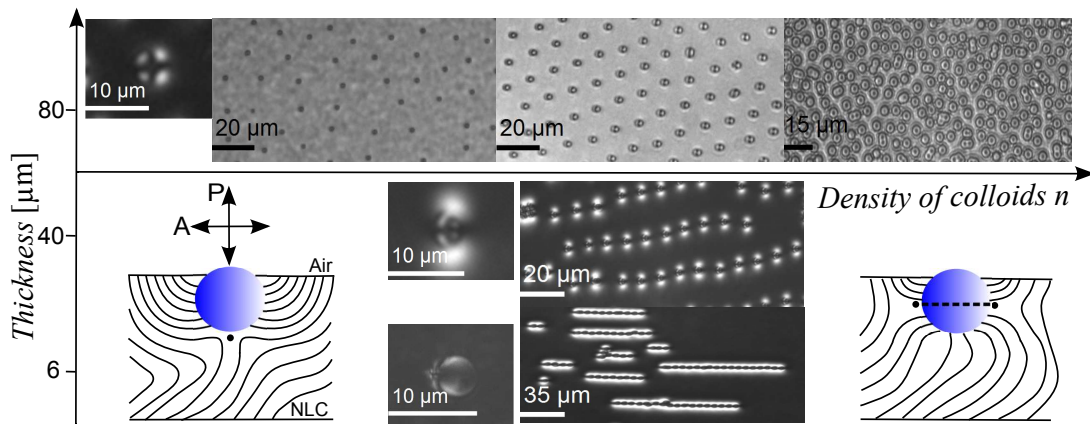


FIG. 2: Patterns formed by $4\mu\text{m}$ diameter colloids trapped at the air/NLC interface when a strong planar anchoring is imposed by the lower substrate. In thin samples, chains form along the direction of alignment. They are not observed at large thicknesses ($d > 40\mu\text{m}$) where the patterns strongly depend on the colloids density, going from a liquid to a loose crystal and an amorphous condensed state. Sketches illustrate two main possible nematic textures around the beads.

equipped with an INSTEC hot stage (temperature regulated at 0.1°C) and a SONY 1024x768 digital camera. Birefringence measurements with a Berek compensator were used to determine the thickness of the thinnest hybrid films. The microscope also allows an accurate characterization of interfaces in reflection mode by Vertical Scanning and Phase Shift Interferometries [21, 22] thanks to a Mirau objective (x20) mounted on a Nano-F (MCL) nanopositionner focusing element. We also used optical tweezers based on a LEICA DMI 3000 B inverted microscope equipped with a x100 (NA 1.4) oil immersion objective, a 1064nm laser (YLM 5W from IPG Photonics) and a piezoelectric XY stage (MCL). Silica beads cannot be directly trapped because of the inappropriate index contrast in 5CB but can nevertheless be manipulated with the 'ghost' effects due to the alignment [23]. Tracking procedures (St Andrews Tracker [24]) were used to determine accurately the beads position.

We first checked with vertical scanning interferometry that the beads were actually trapped at the interface. The top of a sphere is easily located with a Mirau objective and the height contrast h (see Fig.1) with the surrounding fluid additionally gives the contact angle of the beads at the air interface $\theta = \arccos(1 - h/R) = 31(\pm 2)^\circ$. The surrounding fluid is flat without detectable localized deformation (with a typical vertical resolution of a few nanometers). After the sample preparation, beads begin to organize into larger clusters, depending on their area density, the anchoring conditions and the LC layer thickness. The planar case is summarized in Fig. 2. Between crossed polarizers, a point defect close to the bead is always observed in thin layers ($d < 30\mu\text{m}$). It is reminiscent of the hyperbolic defect that forms around beads of micrometer size in planar cells [14]. This defect disappears at large thickness, where the birefringence pattern looks more radial (Maltese Cross in top left). In thin layers,

the beads spontaneously form linear chains parallel to the easy axis. Individual colloids are then attracted by those chains which grow and finally collect all surrounding particles. When the thickness increases, the chains are much less defined and are no more observed typically above $40\mu\text{m}$. At larger thicknesses, the patterns are very sensitive to the area density of deposited colloids. This evolution is shown in the top pictures. At a low colloidal density, a stable liquid behaviour is observed. Increasing the density typically above $1000 \text{ colloids}.\text{mm}^{-2}$, crystalline hexagonal domains appear and form a single crystal in a few hours. If the density is higher (above $10000 \text{ colloids}.\text{mm}^{-2}$), an increasing number of amorphous 2D aggregates (top right picture) are observed in coexistence with the crystalline structure. When the anchoring on the lower substrate is homeotropic the same patterns and density thresholds are observed indicating that the colloids interactions are very similar in a homeotropic slab and in large hybrid layers. These observations are somewhat reminiscent of the hexagonal lattices formed by glycerin droplets at the air-liquid crystal interface [10, 11]. In that case, the liquid structure at low density and the amorphous condensed state at large one are however absent. Two main differences might explain these discrepancies. First the particles we used are solid silica spheres and are not deformed at the interface. Second, the anchoring on DMOAP is strongly homeotropic (the anchoring energy is $W \approx 10^{-2} \text{ J}.\text{m}^{-2}$ [19]) whereas it is planar degenerated on glycerin. The detailed nematic texture still has to be deciphered but two suggestions are sketched in Fig. 2. They are based on observations of beads with homeotropic anchorings dispersed inside nematic planar cells which show the presence of either a hyperbolic hedgehog point defect or a Saturn ring [14].

As said above, the nature of the interactions between colloids trapped at a nematic interface is still debated.

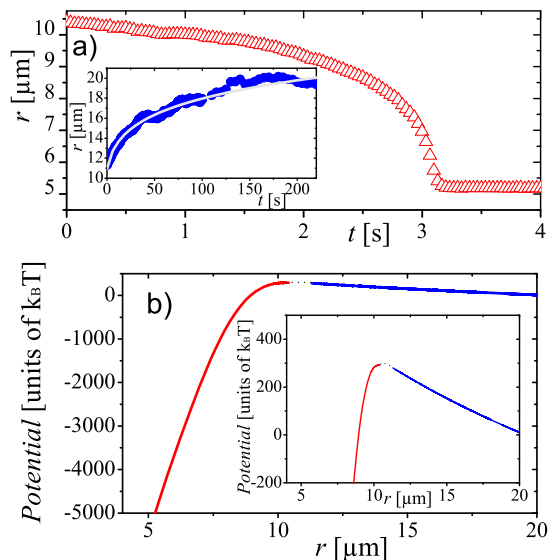


FIG. 3: Time dependence of the separation distance between two isolated particles released at $10.5 \mu\text{m}$ and at $11 \mu\text{m}$ (Inset). (b) Corresponding pair potential (arbitrarily fixed at $k_B T$ at $r=20 \mu\text{m}$) derived from several beads trajectories. Inset: zoom around the unstable equilibrium distance r_a .

The hexagonal lattices of glycerin droplets [10] or microparticles [13] have been explained by the existence of an equilibrium inter-beads distance. The latter results from the nematic elastic repulsion competing with a capillary attraction arising from the nematic pressure on each beads. In a recent paper, Oettel however [17] shows that the weak interface deformation cannot account for the observed effects. The possible role of many-body interactions in stabilizing the structures has also been discussed recently in Ref. [18]. In our case, the nematic elasticity is clearly a key ingredient, since the hexagonal patterns disappear through the nematic-isotropic phase transition. An equilibrium distance between two particles is however hardly compatible with the various observed structures and we focused on the bead-bead pair potential. With optical tweezers, two isolated beads are approached at an initial distance r_o and are tracked after trap release. We show in Fig.3(a) a typical evolution of the separation distance r . As long as r_o is larger than $r_a = 10.5 \pm 0.5 \mu\text{m}$, the beads move away from each other. They irreversibly aggregate for $r_o < r_a$ with a final separation of $1 \mu\text{m}$. Averaged over several trajectories, the interaction force f_p can be obtained from the Stokes law [25], and the pair potential energy E_p by its integration [26]. The latter is given in Fig.3(b). For beads with *homeotropic* anchoring, our observations therefore prove that an *unstable* equilibrium distance r_a separates a region of attraction at short distances, and of repulsion at larger ones. The value of r_a is roughly constant with the thickness (above $40 \mu\text{m}$) and the pair orientation, indicating that the lower planar anchoring is screened by

the homeotropic anchoring on air. Such a pair energy profile differs from the one between two glycerin droplets expected in Ref. [10]. We first checked if the repulsive part between two trapped beads was compatible with a “pure bulk” elastic interaction in a large-distance multipolar development. Whatever the exact nematic texture, the homeotropic anchoring at the air forbids a dipolar distortion [17] around a bead (for textures with cylindrical symmetry). Dimensional analysis yields the following pair potential for the non-zero quadrupole moment [27]:

$$E_p = \frac{36\pi K \beta^2 R^6}{r^5}, \quad (1)$$

where $K \sim 10^{-11} \text{N}$ is the 5CB elastic modulus in the one constant approximation and β a coefficient of order unity. The repulsive trajectory is then given by the competition between the drag force $f_v = -\gamma v = -\gamma \dot{r}/2$ and the driving force $f_p = -\partial E_p / \partial r$:

$$r(t) = (2520\pi K \beta^2 R^6 t / \gamma + r_o^7)^{1/7}. \quad (2)$$

This expression correctly fits the trajectories (Fig. 3-a) with $\beta = 2.1 \pm 0.2$. To explain the short distance attraction, we first examined the simple approach of Ref. [10] that consists in adding a capillary attraction term. The corresponding logarithmic dependence is however overwhelmed by the algebraic elastic dependence at short distance. A more refined approach derived from Ref. [17] yields the same conclusion: an additional capillary attraction is unlikely responsible for the observed attraction. A strong reorganization of the director field could however explain it, as already observed in the short distances binding observed for homeotropically-treated beads in bulk nematic films [28] and also supported by the similitude of the pair potential profile with the one theoretically computed for infinite parallel cylinders located at the nematic/isotropic interface in Ref. [29] where such a reorganization clearly appears at short distances.

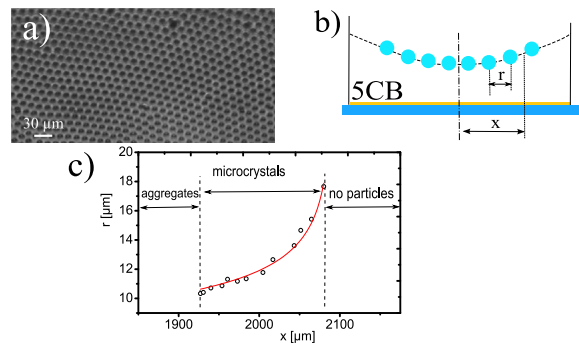


FIG. 4: (a) Optical micrograph of hexagonal crystals at a curved nematic/air interface. (b) Geometry of the experiment (c) Measured separation distance r between colloids as a function of its distance x from center.

The pairwise potential qualitatively explains the structures formed by the trapped beads. At low densities, the mean distance r_m between two beads is much larger than r_a and a liquid is observed. The hexagonal patterns spontaneously form for intermediate densities where $r_a < r_m$) due to the strong inter-beads repulsion. The lattice period is however limited by r_a and for large enough densities ($r_m < r_a$) some particles spontaneously and irreversibly aggregate. Differently from the glycerin droplets case, the period is therefore not univocally defined but changes with area density. To probe if many-body effects strongly influence this scenario, a known additional interaction was applied on the crystals. We used slightly convex air-NLC interfaces resulting from a non perpendicular contact angle on a cylindrical clean glass tube (see Fig. 1-c). After the deposition (at a weak density), the beads converge to the center. After a few days they form stable large crystals with a period depending on the distance x from the center. When more beads are added at the periphery the system reaches a new equilibrium with a decreasing mesh size until aggregates start to form in the center. Figure 4-c shows the lattice period as a function of x . A single amorphous aggregate is observed at the center. Further, the crystal appears with a period close to r_a that rapidly increases up to the crystal end. Such a variation is due to the gravity forces projected onto the interface that oppose the beads' repulsion. The resulting 2D pressure $\Pi = \sqrt{3}f_p/r$ is derived from the inter-beads force in an hexagonal lattice of density $n = 2/\sqrt{3}r^2$. The balance of the forces yields:

$$\Delta m g \sin(\alpha x) n(x) = -\frac{\partial \Pi(x)}{\partial x}, \quad (3)$$

where Δm is the effective mass of a buoyant trapped bead and $\alpha x \ll 1$ the interface slope. Using (1) as the pair potential, we obtain the form

$$r = (A - Bx^2)^{-1/5}, \quad (4)$$

where A is an integration constant and $B = \Delta m g \alpha / 756 \pi K \beta^2 R^6$. This expression fits the data with $B \approx 1.1 \times 10^{31} \text{ m}^{-7}$ (Fig.4-c) while we measured $\alpha = 92.2 \text{ m}^{-1}$. Although this result yields a slightly smaller value $\beta \approx 1.4$ when taking for densities $\rho_{beads} \approx 2 \text{ g.cm}^{-3}$ (provided by Bangslabs) and $\rho_{5CB} \approx 1 \text{ g.cm}^{-3}$, we can conclude that the pairwise potential is enough to describe the observed patterns at least in a first approximation.

In conclusion, we have exhaustively described the behavior of microparticles with a homeotropic anchoring at a nematic/air interface and reported on the first direct measurements of the corresponding pairwise interaction. The latter is found attractive at short distances and repulsive at large ones. The long-range repulsive part is compatible with an elastic quadrupolar interaction. It satisfactory accounts for the hexagonal crystals we observed under simple or gravitational confinement. This

same repulsive interaction could also be at the origin of the recently observed crystals at LC/water interface [13]. The origin of the attractive part is still an open question. The measured flatness of the interface and the expected spatial dependency of the capillary interaction suggest it also has an elastic origin. One possible mechanism of this all-elastic interaction from repulsion to attraction could be related to a defect transformation with consequent colloidal binding. We are confident that this work will stimulate further experimental and theoretical studies to elucidate these fascinating interfacial phenomena.

This work was supported in part by French ANR grant BLAN07-1.183526 "Surfoids". The authors also thank M. Abkarian for fruitful discussions.

* Electronic address: nobili@lcvn.univ-montp2.fr

† Electronic address: blanc@lcvn.univ-montp2.fr

- [1] U. Gasser *et al.*, ChemPhysChem., **11**, 963 (2010).
- [2] B. P. Binks, Phys. Chem. Chem. Phys., **9**, 6298 (2007).
- [3] P. Pierensky, Phys. Rev. Lett., **45**, 569 (1980).
- [4] T. Terao and T. Nkayama, Phys. Rev. E, **60**, 7157 (1999).
- [5] A. D. Dinsmore *et al.*, Science, **298**, 1006 (2002).
- [6] K. D. Danov, and P. A. Kralchevsky, J. Colloid Interf. Sci. **345**, 505 (2010).
- [7] B. J. Park *et al.*, Langmuir, **24**, 1686 (2008).
- [8] E. Nouruzifar, and M. Oettel, Phys. Rev. E, **79**, 051401 (2009).
- [9] K. D. Danov, and P. A. Kralchevsky, Adv. Colloid Interface Sci. **154**, 91 (2010).
- [10] I. I. Smalyukh *et al.*, Phys. Rev. Lett. **93**, 117801 (2004).
- [11] A. B. Nych *et al.*, Phys. Rev. Lett. **98**, 057801 (2008).
- [12] I. H. Lin *et al.*, J. Phys. Chem. B **112**, 16552 (2008).
- [13] G. M. Koeing *et al.*, Proc. Natl. Acad. Sci. USA **107**, 3998 (2010).
- [14] P. Poulin and D. A. Weitz, Phys. Rev. E **57**, 626 (1998).
- [15] P. Poulin *et al.*, Nature **275**, 1770 (1997).
- [16] T. Yamamoto, and M. Yoshida, Appl. Phys. Express **2**, 101501 (2009).
- [17] M. Oettel *et al.*, Eur. Phys. J. E **28**, 99 (2009).
- [18] V. M. Pergamenschchik, Phys. Rev. E **79**, 011407 (2009).
- [19] M. Škarabot *et al.*, Phys. Rev. E **77**, 031705 (2008).
- [20] The anchoring was checked by dispersing some beads in a planar 5CB cell where colloidal chains and distinctive birefringence spontaneously patterns form [14, 19].
- [21] P. J. Caber, Appl. Opt. **32**, 3438 (1993).
- [22] B. Bhushan, J. C. Wyant and C. Koliopoulos, Appl. Opt. **24**, 1489 (1985).
- [23] I. Mušević *et al.*, Phys. Rev. Lett. **93**, 187801 (2004).
- [24] C. Lopez-Mariscal *et al.*, Opt. Express **14**, 4182 (2006).
- [25] The Stokes's law $f = \gamma v$ acting at the velocity v is determined from the diffusion coefficient $D = k_B T / \gamma$ obtained from the mean squared displacement of an isolated bead.
- [26] M. Škarabot *et al.*, Phys. Rev. E **76**, 051406 (2007).
- [27] T. C. Lubensky *et al.*, Phys. Rev. E **57**, 610 (1998).
- [28] I. Mušević *et al.*, Science **313**, 954 (2006).
- [29] D. Andrienko, M. Tasinkevych, and S. Dietrich, Europhys. Lett., **70**, 95 (2005).